New discrete and polymeric supramolecular architectures derived from dinuclear Co(II), Ni(II) and Cu(II) complexes of aryl-linked bis-β-diketonato ligands and nitrogen bases: synthetic, structural and high pressure studies†

Jack K. Clegg,[a] Michael J. Hayter,[a] Katrina A. Jolliffe,[a] Leonard F. Lindoy,*[a] John C. McMurtrie,[b] George V. Meehan,[c] Suzanne M. Neville,[a] Simon Parsons,[d,e] Peter A. Tasker,[e] Peter Turner[a] and Fraser J. White[d,e]

Received 29th September 2009, Accepted 4th December 2009
First published as an Advance Article on the web 2nd February 2010
DOI: 10.1039/b920199h

New examples of nitrogen base adducts of dinuclear Co(II), Ni(II) and Cu(II) complexes of the doubly deprotonated forms of 1,3-aryl linked bis-β-diketones of type [RC(=O)CH_2C(=O)C_6H_4C(=O)CH_2C(=O)R] (L^1H_2) incorporating the mono- and difunctional amine bases pyridine (Py), 4-ethylpyridine (EtPy), piperidine (pipi), 1,4-piperazine (pip), *N*-methylmorpholine (mmorph), 1,4-dimethylpiperazine (dmpip) and *N*,*N*,*N*′,*N*′-tetramethylethylenediamine (tmen) have been synthesised by reaction of the previously reported $[Cu_2(L^1)_2]\cdot 2.5THF$ (R = Me), $[Cu_2(L^1)_2(THF)_2]$ (R = *t*-Bu), $[Ni_2(L^1)_2(Py)_4]$ (R = *t*-Bu) and $[Co_2(L^1)_2(Py)_4]$ (R = *t*-Bu) complexes with individual bases of the above type. Comparative X-ray structural studies involving all ten base adduct derivatives have been obtained and reveal a range of interesting discrete and polymeric molecular architectures. The respective products have the following stoichiometries: $[Cu_2(L^1)_2(Py)_2]\cdot Py$ (R = Me), $[Cu_2(L^1)_2(EtPy)_2]\cdot 2EtPy$ (R = *t*-Bu), $[Cu_2(L^1)_2(pipi)_2]\cdot 2pipi$ (R = *t*-Bu), $[Cu_2(L^1)_2(mmorph)_2]$ (R = *t*-Bu), $[Cu_2(L^1)_2(tmen)_2]$ (R = *t*-Bu) and $\{[Cu_2(L^1)_2(pip)]\cdot pip\cdot 2THF\}_n$, $[Co_2(L^1)_2(tmen)_2]$ (R = *t*-Bu), $[Ni_2(L^1)_2(Py)_4]\cdot dmpip$ (R = *t*-Bu), $[Ni_2(L^1)_2(pipi)_4]\cdot pipi$ (R = *t*-Bu) and $[Ni_2(L^1)_2(tmen)_2]$ (R = *t*-Bu). The effect of pressure on the X-ray structure of $[Cu_2(L^1)_2(mmorph)_2]$ has been investigated. An increase in pressure from ambient to 9.1 kbar resulted in modest changes to the unit cell parameters as well as a corresponding decrease of 6.7 percent in the unit cell volume. While a small 'shearing' motion occurs between adjacent molecular units throughout the lattice, no existing bonds are broken or new bonds formed.

Introduction

The interaction of β-diketone ligands with metals from across the Periodic Table has been investigated since the beginning of the twentieth century[1] while the metallo-supramolecular chemistry of β-diketone derivatives[2] (and related malonate analogues)[3,4] has been explored more recently.[4] In particular, there has been much interest in systems in which more than one β-diketone motif have been incorporated into supramolecular architectures.[5] We[6-13] and others[15,16] have demonstrated the versatility of such systems in the formation of a variety of neutral triangles,[6,8,13,16] triple helices,[7] tetrahedra[6] and capsules.[14] A number of linked extended structures including infinite trigonal prisms,[8] tetranuclear 'dimers of dimers'[7,9] and a variety of coordination polymeric systems have been reported.[7-9] We have found that use of the semi-rigid geometries of the sp^2-hybridised ligands L^1 and L^2 has allowed a level of predictability in the formation of particular structures when combined with metal ions with preferred coordination geometries. Of particular note, was the demonstration that the neutral (often solvated) species of type $[Cu_2(L^1)_2]$ (**1**) and $[Cu_3(L^2)_3]$ (**2**) can be employed as essentially planar 'platform' building blocks for the facile formation of new extended multinuclear arrays, often displaying unusual architectures, when reacted with appropriate difunctional heterocyclic nitrogen (ancillary) ligands. Motivated by these results, we now report an extension of these studies that involved the interaction of new Co(II), Ni(II) and Cu(II) dinuclear species of type **1** with selected monofunctional and difunctional heterocyclic nitrogen ligands (see Scheme 1). An aim of this study has been to probe the generality (or otherwise) of the prior results for Cu(II), while widening the investigation to include the interaction of the dinuclear complexes of both Co(II) and Ni(II) with the extended range of ancillary ligands just mentioned.

Experimental

All reagents and solvents were purchased from commercial sources. Tetrahydrofuran (THF) was pre-dried over sodium wire before use. NMR spectra were recorded on Bruker Avance DPX200, DPX300 or DPX400 spectrometers; δ_H values are

[a]*School of Chemistry, University of Sydney, NSW, 2006, Australia*
[b]*School of Physical and Chemical Sciences, Queensland University of Technology, GPO Box 2434, Brisbane, 4001, Australia*
[c]*School of Pharmacy and Molecular Sciences, James Cook University, Townsville, Qld, 4814, Australia*
[d]*Centre for Science at Extreme Conditions, University of Edinburgh, Edinburgh, EH9 3JZ, UK*
[e]*School of Chemistry, University of Edinburgh, Edinburgh, EH9 3JJ, UK*

† Electronic supplementary information (ESI) available: Experimental details. CCDC reference numbers 754701–754713. For ESI and crystallographic data in CIF or other electronic format see DOI: 10.1039/b920199h

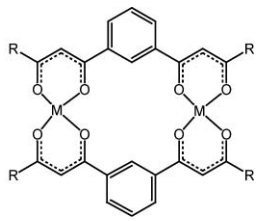

1 $[M_2(L^1)_2]$ R = Me, Et, Pr, ^{t}Bu, hexyl, octyl, nonyl

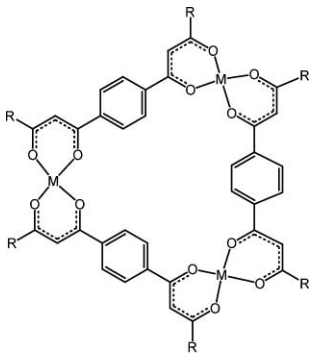

2 $[M_3(L^2)_3]$ R = Me, Et, Pr, ^{t}Bu, hexyl, octyl, nonyl

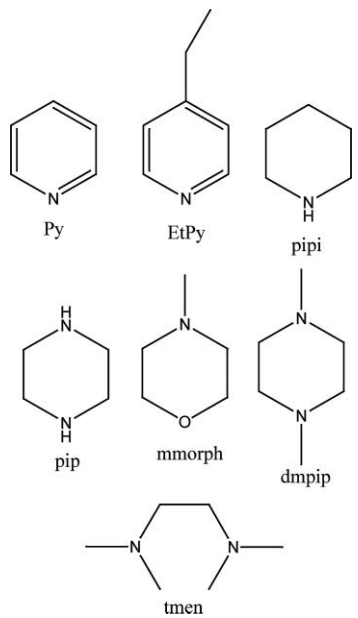

Scheme 1 Ancillary ligands used in the study.

relative to Me_4Si at 0 ppm. Low resolution electrospray ionisation mass spectra (ESI-MS) were obtained on a Finnigan LCQ-8 spectrometer. FTIR (KBr) spectra were collected using a Bio-Rad FTS-40 spectrometer. UV-vis solid state spectra were recorded on a Cary 1E spectrophotometer in the solid state.

Ligand synthesis

Ligands H_2L^1 (R = Me and *t*-Bu) were prepared and characterised as described previously.[7]

Complex synthesis

$[Cu_2(L^1)_2]\cdot 2.5THF$ (R = Me), $[Cu_2(L^1)_2(THF)_2]$ (R = *t*-Bu), $[Ni_2(L^1)_2(Py)_4]$ (R = *t*-Bu) and $[Co_2(L^1)_2(Py)_4]$ (R = *t*-Bu) were synthesised and characterised as described previously.[7,11] Individual products were washed with ether prior to microanalysis; crystalline samples used for microanalysis were first crushed and then allowed to stand in air prior to analysis. As observed previously for related complex species,[7] in some cases the adduct complexes rapidly lost their axial ligands on removal from the reaction solution. When this occurred, a crystal of the product was transferred quickly to the diffractometer, cooled in the cryostream, and the structure determined in the absence of further characterisation of the complex.

$[Cu_2(L^1)_2(Py)_2]\cdot$Py (R = Me) and $[Cu_2(L^1)_2(EtPy)]\cdot 1.5$EtPy (R = *t*-Bu). Four equivalents of pyridine (Py) or 4-ethylpyridine (EtPy) (2.0 mmol) in warm THF (10 mL) were added to the appropriate Cu(II) complex of L^1 (0.50 mmol) in warm tetrahydrofuran (40 mL). The resulting dark green solution was stirred for 1 h and the colour changed to bright green. The reaction mixture was then allowed to cool to room temperature before filtration. Crystals were obtained in each case upon evaporation of the tetrahydrofuran filtrate over several days.

$[Cu_2(L^1)_2(Py)_2]\cdot$Py (R = Me): This complex rapidly loses pyridine in air. A single crystal was removed from the reaction solution and used directly for the crystallographic study.

$[Cu_2(L^1)_2(EtPy)]\cdot 1.5$EtPy (R = *t*-Bu): Yield 182 mg (60%), green crystals. Found: C, 66.43; H, 6.77; N, 4.50%. Calc. for $C_{54}H_{66}Cu_2N_2O_8\cdot 1.5(C_7H_9N)$: C, 66.84; H, 6.91; N, 4.23%. UV-Vis (solid state): 360, 468, 684 nm. A single crystal was removed directly from the reaction solution and used for the X-ray study; the structure determination indicated a stoichiometry of $[Cu_2(L^1)_2(EtPy)_2]\cdot 2$EtPy (R = *t*-Bu).

$\{[Cu_2(L^1)_2(pip)]\cdot pip\cdot 2THF\}_n$ (R = *t*-Bu). One equivalent (0.1 mmol) of piperazine was added to a warm stirred solution of $[Cu_2(L^1)_2(THF)_2]$ (R = *t*-Bu) (0.1 mmol) of L^1 in tetrahydrofuran (40 mL). The reaction mixture was brought to reflux and was then allowed to cool to room temperature, the solution was filtered and the filtrate left to stand. A small number of air unstable green crystals grew on slow evaporation of the reaction mixture; one of these was used directly for the crystallographic study.

$[Co_2(L^1)_2(tmen)_2]$ (R = *t*-Bu), $[Ni_2(L^1)_2(Py)_4]\cdot$dmpip (R = *t*-Bu), $[Ni_2(L^1)_2(tmen)_2]$ (R = *t*-Bu), $[Ni_2(L^1)_2(pipi)_4]\cdot$pipi (R = *t*-Bu), $[Cu_2(L^1)_2(tmen)_2]$ (R = *t*-Bu), $[Cu_2(L^1)_2(pipi)_2]\cdot 2$pipi (R = *t*-Bu). The required metal complex (10 mg, 0.01 mmol) of L^1 was dissolved in a warm solution (5 mL) of the desired auxiliary ligand. The solution was brought to reflux, filtered, and the filtrate allowed to cool slowly. In each case a small number of crystals grew on slow evaporation of the reaction mixture; a single crystal from each of these solutions was used directly for the respective crystallographic studies.

$[(Cu_2(L^1)_2(mmorph)_2]\cdot 2H_2O$ (R = *t*-Bu). A similar procedure to that described above starting from $[Cu_2(L^1)_2(THF)_2]$ (R = *t*-Bu) yielded dark green crystals that were isolated and dried in air. Yield 9.5 mg (93%). Found: C, 58.99; H, 7.23; N, 2.88. Calc. for $C_{50}H_{70}Cu_2O_{10}N_2\cdot 2H_2O$: C, 58.75; H, 7.30; N, 2.73%. The

X-ray structure of a crystal taken directly from the reaction solution yielded the formula $[(Cu_2(\mathbf{L}^1)_2(mmorph)_2]$ (R = *t*-Bu).

X-ray structure determinations

Ambient pressure studies. Data for $[Ni_2(\mathbf{L}^1)_2(Py)_4]\cdot dmpip$ (R = *t*-Bu) and $[Cu_2(\mathbf{L}^1)_2(tmen)_2]$ (R = *t*-Bu) were collected on a Bruker SMART 1000 diffractometer employing graphite-monochromated Mo-Kα radiation generated from a sealed tube (0.71073 Å) with ω scans.[17] Structural data for the other complexes, were collected on a Bruker-Nonius APEXII-X8-FR591 diffractometer employing graphite-monochromated Mo-Kα radiation generated from a rotating anode (0.71073 Å) with ω and ψ scans.[18] All data were collected to approximately 56° 2θ at 150(2) K except where otherwise indicated. Data integration and reduction were undertaken with SAINT and XPREP[19] and subsequent computations were carried out using the WinGX-32 graphical user interface.[20] Structures were solved by direct methods using SIR97.[21] Multi-scan empirical absorption corrections were applied to data sets using the program SADABS.[22] Data were refined and extended with SHELXL-97.[23] In general, non-hydrogen atoms with occupancies greater than 0.5 were refined anisotropically. Carbon-bound hydrogen atoms were included in idealised positions and refined using a riding model. Nitrogen bound hydrogen atoms were located in the difference Fourier map before refinement.

Elevated pressure studies. High-pressure X-ray studies were carried out using a modified Merrill–Bassett diamond-anvil cell (half-opening angle 40°), equipped with brilliant cut diamonds with 600 μm culets and a tungsten gasket.[24] The hydrostatic medium employed was paraffin oil and a small ruby chip was also loaded into the cell so that the pressure could be monitored using the ruby fluorescence method.[25] Data were collected employing silicon monochromated synchrotron radiation (0.4920 Å) using a Bruker-Nonius APEX II CCD diffractometer on station 9.8 at CCLRC SRS Daresbury Laboratory. Data collection and processing procedures followed those previously reported.[26] Data integration and reduction were undertaken with SAINT and XPREP,[19] and absorption corrections with the programs SHADE,[27] SADABS[22] and merging was carried out with SORTAV[28] with robust-resistant weights.[29] Structures were solved by direct methods using SIR97.[21] Data were refined and extended with both CRYSTALS[30] and SHELXL-97.[23] Because of low completeness of the data sets, refinement of phenylene rings and *t*-butyl groups were carried out with rigid body restraints and all other C–C, C–O and C–N bond lengths were restrained. All non-hydrogen atoms with occupancies of greater than 0.5 were refined anisotropically with a variety of restraints and constraints required to facilitate realistic modelling. Carbon-bound hydrogen atoms were included in idealised positions and refined using a riding model.

Crystal data. Crystal and structure refinement data for ambient pressure and high pressure structures are summarised in Tables 1 and 2. Depictions of the crystal structures are provided in Fig. 1–13. The ESI contains further details relating to the X-ray crystal structure refinements as well as tables of selected bond lengths and angles and hydrogen bonding geometries.†

Results and discussion

During the course of the present investigation the following ten new complexes were synthesised, $[Cu_2(\mathbf{L}^1)_2(Py)_2]\cdot Py$ (R = Me), $[Cu_2(\mathbf{L}^1)_2(EtPy)_2]\cdot 2EtPy$ (R = *t*-Bu), $[Cu_2(\mathbf{L}^1)_2(pipi)_2]\cdot 2pipi$ (R = *t*-Bu), $[Cu_2(\mathbf{L}^1)_2(mmorph)_2]$ (R = *t*-Bu), $[Cu_2(\mathbf{L}^1)_2(tmen)_2]$ (R = *t*-Bu) and $\{[Cu_2(\mathbf{L}^1)_2(pip)]\cdot pip\cdot 2THF\}_n$, $[Co_2(\mathbf{L}^1)_2(tmen)_2]$ (R = *t*-Bu), $[Ni_2(\mathbf{L}^1)_2(Py)_4]\cdot dmpip$ (R = *t*-Bu), $[Ni_2(\mathbf{L}^1)_2(pipi)_4]\cdot pipi$ (R = *t*-Bu), $[Ni_2(\mathbf{L}^1)_2(tmen)_2]$ (R = *t*-Bu), and their structures determined by X-ray diffraction.

$[Cu_2(\mathbf{L}^1)_2(Py)_2]\cdot Py$ (R = Me) was obtained as green prismatic crystals after several days of slow evaporation of the corresponding reaction mixture. An ORTEP plot of the structure is given in Fig. 1. As expected, the copper atoms are five-coordinate, with the fifth site occupied by pyridine ligands. Overall the structure is similar to that of $[Cu_2(\mathbf{L}^1)_2(Py)_2]\cdot Py$ (R = *t*-Bu) reported previously.[7] In both structures the two coordinated pyridine molecules are orientated mutually *trans* across the mean plane of each molecule and each Cu(II) ion exhibits a distorted square pyramidal geometry. However, the degree to which the Cu(II) ion is distorted from the square pyramidal geometry is different in each structure. For $[Cu_2(\mathbf{L}^1)_2(Py)_2]\cdot Py$ (R = *t*-Bu), the Cu(II) ions deviate from the mean plane of the molecule (calculated including all oxygen atoms) by 0.1753(7) Å; however, the corresponding deviation in $[Cu_2(\mathbf{L}^1)_2(Py)_2]\cdot Py$ (R = Me) is greater at 0.2583(7) Å. This is also reflected by a slightly smaller distance (6.75(1) Å) between the methyl groups of each $\mathbf{L}^1$ in $[Cu_2(\mathbf{L}^1)_2(Py)_2]\cdot Py$ (R = Me) complex relative to the distance

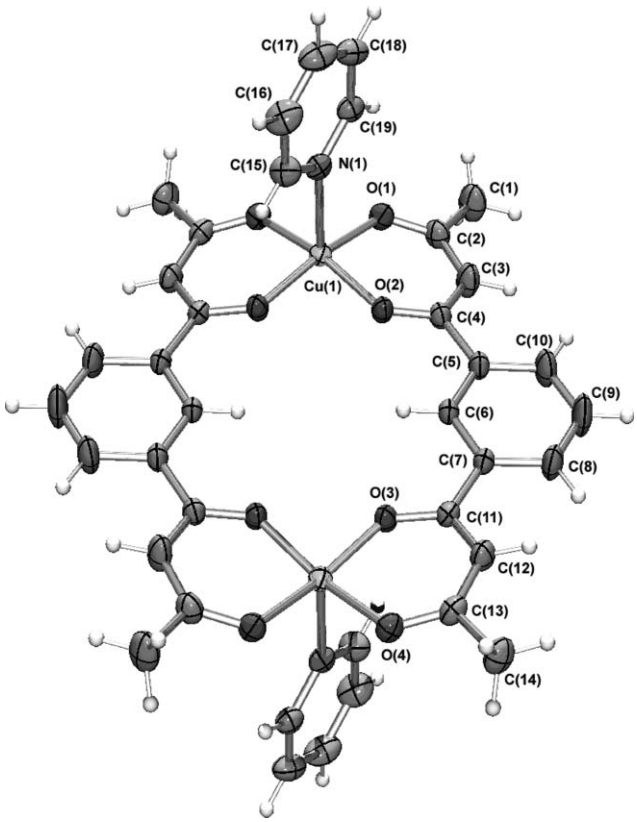

Fig. 1 ORTEP plot of $[Cu_2(\mathbf{L}^1)_2(Py)_2]\cdot Py$ (R = Me), shown with 50% probability ellipsoids. Solvate molecules are omitted for clarity. Symmetry code used to generate equivalent atoms: –x, –y, –z.

Table 1 Crystal and structure refinement data for the ambient pressure metal complexes reported

Compound	$[Cu_2(\mathbf{L}^1)_2(Py)_2]\cdot Py$ (R = Me)	$[Cu_2(\mathbf{L}^1)_2(EtPy)]\cdot 2EtPy$ (R = *t*-Bu)	$[Ni_2(\mathbf{L}^1)_2(pipi)_4]\cdot pipi$ (R = *t*-Bu)	$[Cu_2(\mathbf{L}^1)_2(pipi)_2]\cdot pipi$ (R = *t*-Bu)	$[Co_2(\mathbf{L}^1)_2(tmen)_2]$ (R = *t*-Bu)	$[Ni_2(\mathbf{L}^1)_2(tmen)_2]$ (R = *t*-Bu)	$[Cu_2(\mathbf{L}^1)_2(tmen)_2$ (R = *t*-Bu)	$[Ni_2(\mathbf{L}^1)_2(Py)_4]\cdot dmpip$ (R = *t*-Bu)	$\{[Cu_2(\mathbf{L}^1)_2(pip)]\cdot pip\cdot 2THF\}_n$ (R = *t*-Bu)
Formula of Refinement Model	$C_{43}H_{39}Cu_2N_3O_8$	$C_{68}H_{84}Cu_2N_4O_8$	$C_{65}H_{103}N_5Ni_2O_8$	$C_{60}H_{92}Cu_2N_4O_8$	$C_{52}H_{80}Co_2N_4O_8$	$C_{52}H_{80}N_4Ni_2O_8$	$C_{52}H_{80}Cu_2N_4O_8$	$C_{66}H_{82}N_6Ni_2O_8$	$C_{28}H_{42}CuN_2O_5$
Molecular Weight	852.85	1212.47	1202.81	1124.46	1007.06	1006.62	1016.28	1204.76	550.18
Crystal System	Triclinic	Triclinic	Monoclinic	Monoclinic	Monoclinic	Monoclinic	Triclinic	Triclinic	Triclinic
Space Group	$P\bar{1}$ (#2)	$P\bar{1}$ (#2)	$P2_1/n$ (#14)	$C2/m$ (#12)	$C2/c$ (#15)	$C2/c$ (#15)	$P\bar{1}$ (#2)	$P\bar{1}$ (#2)	$P\bar{1}$ (#2)
a/Å	8.298(1)	11.013(1)	22.411(3)	9.9434(4)	29.6686(16)	29.799(5)	9.4163(10)	9.206(5)	10.340(5)
b/Å	8.795(1)	11.390(1)	10.9718(15)	19.2818(7)	10.3395(7)	10.3542(15	10.5103(11)	11.144(6)	11.737(6)
c/Å	14.0240(11)	13.365(1)	27.490(4)	15.7332(6)	19.7231(10)	19.542(3)	15.2349(16)	16.107(8)	12.916(6)
α (°)	76.427(4)	81.312(2)	90	90	90	90	95.511(2)	74.619(8)	95.039(8)
β (°)	85.101(4)	78.572(2)	101.990(2)	97.706(2)	114.835(3)	114.693(11)	94.794(2)	79.261(9)	113.367(7)
γ (°)	72.381(4)	76.639(2)	90	90	90	90	115.995(2)	83.014(9)	98.987(8)
V/Å^3	948.12(18)	1589.0(2)	6612.0(15)	2989.2(2)	5490.7(6)	5478.2(16)	1335.6(2)	1560.8(13)	1401.8(11)
Dc/g cm^{-3}	1.494	1.267	1.205	1.249	1.218	1.220	1.264	1.282	1.303
Z	1	1	4	2	4	4	1	1	2
Crystal Size/mm	0.208 × 0.171 × 0.081	0.373 × 0.290 × 0.110	0.280 × 0.100 × 0.080	0.260 × 0.180 × 0.070	0.290 × 0.280 × 0.100	0.190 × 0.180 × 0.080	0.450 × 0.450 × 0.250	0.450 × 0.200 × 0.100	0.280 × 0.150 × 0.020
Crystal Colour	Green	Green	Green	Green	Orange	Green	Green	Green	Green
Crystal Habit	Block	Prism	Needle	Blade	Block	Block	Plate	Needle	Plate
μ(Mo-Kα)/mm^{-1}	0.898	0.726	0.624	0.766	0.656	0.739	0.850	0.662	0.818
T(Empirical)$_{min,max}$	0.712, 0.91	0.572, 0.923	0.828, 0.951	0.876, 0.948	0.878, 0.937	0.798, 0.943	0.729, 0.809	0.852, 0.936	0.880, 0.984
$2\theta_{max}$ (°)	61.02	61.10	50.64	56.56	56.54	50.00	56.72	57.02	56.98
hkl range	−11 11, −12 12, −20 20	−15 15, −16 16, −19 19	−26 26, −13 13, −33 33	−13 12, −25 23, −20 20	−39 39, −13 13, −25 26	−35 35, −12 12, −23 23	−12 12, −14 14, −19 20	−12 12, −14 14, −21 20	−13 13, −15 15, −16 17
N (N_{var})	17585 (254)	58035 (360)	53078 (770)	17063 (177)	32042 (303)	32516(296)	13260(299)	15431(337)	14064(334)
N_{ind} (R_{merge})	5703(0.0331)	9598 (0.0668)	12025 (0.0853)	3789(0.0446)	6799 (0.0941)	4820(0.1695)	6212(0.0168)	7242(0.0345)	6574(0.0375)
$N_{obs} - (I > 2\sigma(I))$	4670	6904	7701	3048	3962	2550	5711	5031	4826
R_1 [a]- ($I > 2\sigma(I)$), $wR2$ [a]- (all)	0.0349, 0.0960	0.0779, 0.2267	0.0501, 0.1136	0.0630, 0.1522	0.0532, 0.1343	0.0600, 0.1347	0.0372, 0.1049	0.0468, 0.1095	0.0528, 0.1412
A^a, B^a	0.0443, 0.4330	0.1135, 2.4257	0.0484, 0.8661	0.0489, 16.1580	0.0539, 5.4719	0.0616, 0.0000	0.0595, 0.8582	0.0494, 0.2397	0.0742, 0.5502
GoF	1.035	1.101	1.035	1.071	1.002	0.937	1.042	1.005	1.025
Residual Extrema/e$^-$ Å^{-3}	−0.495, 0.534	−1.958, 3.034	−0.269, 0.662	−1.266, 1.511	−0.519, 0.522	−0.523, 0.408	−0.559, 0.782	−0.277, 0.536	−0.865, 0.798

[a] $R1 = \sum||F_o| - |F_c||/\sum|F_o|$ for $F_o > 2\sigma(F_o)$ and $wR2 = \{\sum[w(F_o^2 - F_c^2)^2]/\sum[w(F_c^2)^2]\}^{1/2}$ where $w = 1/[\sigma^2(F_o^2) + (AP)^2 + BP]$, $P = (F_o^2 + 2F_c^2)/3$ and A and B are listed in the crystal data information supplied.

Table 2 Crystal and structure refinement data for $[Cu_2(\mathbf{L}^1)_2(mmorph)_2]$ (R = *t*-Bu)

Pressure	Ambient	Ambient	1.9 kbar	9.1 kbar
Formula of Refinement Model	$C_{50}H_{70}Cu_2N_2O_{10}$	$C_{50}H_{70}Cu_2N_2O_{10}$	$C_{50}H_{70}Cu_2N_2O_{10}$	$C_{50}H_{70}Cu_2N_2O_{10}$
Molecular Weight	986.16	986.16	986.16	986.16
Crystal System	Triclinic	Triclinic	Triclinic	Triclinic
Space Group	$P\bar{1}$(#2)	$P\bar{1}$(#2)	$P\bar{1}$(#2)	$P\bar{1}$(#2)
a/Å	6.9932(5)	7.108(4)	6.9932(11)	6.8237(5)
b/Å	11.2678(9)	11.354(6)	11.2678(18)	11.0237(8)
c/Å	16.4656(14)	16.593(9)	16.466(7)	16.053(3)
α (°)	83.877(7)	82.904(8)	83.88(2)	84.420(12)
β (°)	84.620(5)	84.495(8)	84.62(2)	85.462(12)
γ (°)	73.405(6)	72.746(8)	73.405(11)	73.617(5)
V/Å^3	1233.59(17)	1266.5(11)	1233.6(6)	1151.3(3)
D_x/Mg m^{-3}	1.327	1.293	1.327	1.422
Z	1	1	1	1
Crystal Size/mm	0.35 × 0.08 × 0.01	0.01 × 0.06 × 0.23	0.10 × 0.20 × 0.20	0.10 × 0.20 × 0.20
Crystal Colour	Blue	Blue	Green	Green
Crystal Habit	Blade	Blade	Block	Block
μ/mm^{-1}	0.920	0.896	0.920	0.985
T(Empirical)$_{min,max}$	0.736, 1.000	0.736, 0.991	0.10, 0.92	0.11, 0.91
Wavelength, λ	0.71073	0.71073	0.4920	0.4920
$2\theta_{max}$ (°)	56.68	56.74	34	33.6
T/K	150(2)	293(2)	293(2)	293(2)
N (N_{var})	29756(296)	8318 (296)	5388 (290)	5006 (290)
N_{ind} (R_{merge})	6109(0.0709)	5499 (0.0530)	1732 (0.070)	1553 (0.082)
N_{obs} – ($I > 2\sigma(I)$)	4236	2804	1177	1231
R_1 [a]- ($I > 2\sigma(I)$), *wR2* [a]- (all)	0.0477, 0.1143	0.0723, 0.1540	0.0891, 0.0992	0.0567, 0.0653
GoF	1.051	1.037	1.169	1.181
Residual Extrema/e$^-$ Å^{-3}	–0.826, 0.630	0.437, –0.515	0.35, –0.32	0.29, –0.28

(6.82(1) Å) between the quaternary carbons of the *t*-butyl groups in $[Cu_2(\mathbf{L}^1)_2(Py)_2]\cdot Py$ (R = *t*-Bu). Interestingly, the above differences are not as pronounced as those observed for the previously reported related Zn(II) complexes,[11] $[Zn_2(\mathbf{L}^1)_2(EtPy)_2]$ (R = Me) and $[Zn_2(\mathbf{L}^1)_2(EtPy)_4]$ (R = *t*-Bu), which while synthesised under identical conditions exhibit distorted trigonal bipyramidal and octahedral coordination geometries, respectively. The difference in this case was attributed to the effect of steric factors arising from the difference in bulkiness of the terminal R-groups of the respective ligands.

In an extension of the above study, an identical synthetic procedure to that used for $[Cu_2(\mathbf{L}^1)_2(Py)_2]\cdot Py$ (R = Me) was again carried out except that 4-ethylpyridine was substituted for pyridine as the heterocyclic nitrogen base. The X-ray structure of the resulting crystals indicated a formula of $[Cu_2(\mathbf{L}^1)_2(EtPy)_2]\cdot 2EtPy$ (R = *t*-Bu). The structure (Fig. 2) is generally similar to that of $[Cu_2(\mathbf{L}^1)_2(Py)_2]\cdot Py$ (R = *t*-Bu),[7] except that there is an additional solvent molecule in the lattice. Each Cu(II) ion in this case deviates 0.1857(13) Å from the mean O_8-donor plane (towards the corresponding axial ligand). The uncoordinated 4-ethylpyridine solvent molecules π-stack in an edge-to-face geometry, with the 4-ethylpyridine ligands bound to the copper centres; the CH–π distances fall in the range of 2.8–3.3 Å.

It is noted that the corresponding 4-(dimethylamino)pyridine base has been shown previously by us[7] to interact with $[Cu_2(\mathbf{L}^1)_2]$ (R = *t*-Bu) to yield a similar complex to the above, although the degree of lattice solvation once again differed.

Crystals of $[Ni_2(\mathbf{L}^1)_2(pipi)_4]\cdot pipi$ (R = *t*-Bu) and $[Cu_2(\mathbf{L}^1)_2(pipi)_2]\cdot pipi$ (R = *t*-Bu), incorporating the flexible aliphatic base piperidine (pipi), were grown from a solution of this base and the X-ray structures of each product determined. While the use of flexible components for the construction of supramolecular architectures typically creates additional unpredictability concerning the geometry of the target assembly,[31,32] such systems may yield structures (as well as functions) that are inaccessible when rigid components alone are employed.[33] In this context it is noted that the energetics of conformer interchange of such simple systems is normally small,[34] with (of course) the chair forms being normally favoured. The use of piperidine incorporating sp^3-hybridised NH amine groups as a ligand also introduces the potential for this group to act as a hydrogen bond donor, with each of the four main conformers of piperidine (CA, CE, BA, BE in Fig. 3) potentially giving rise to different coordination and hydrogen bonding vectors.[35]

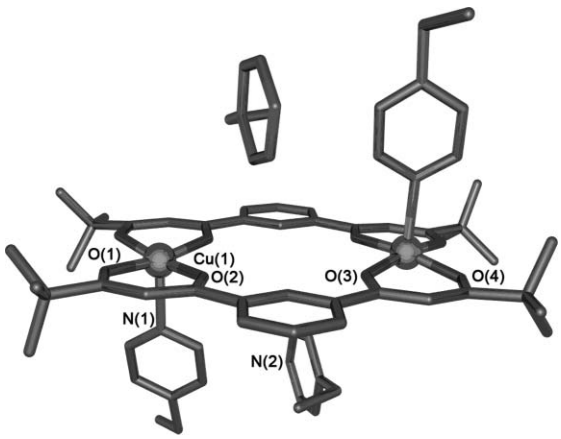

Fig. 2 Perspective representation of the crystal structure of $[Cu_2(\mathbf{L}^1)_2(EtPy)_2]\cdot 2EtPy$ (R = *t*-Bu). There are π–π interactions between the adjacent metal bound and lattice 4-ethylpyridine molecules. Symmetry code used for generating equivalent atoms: –x, 1–y, 1–z.

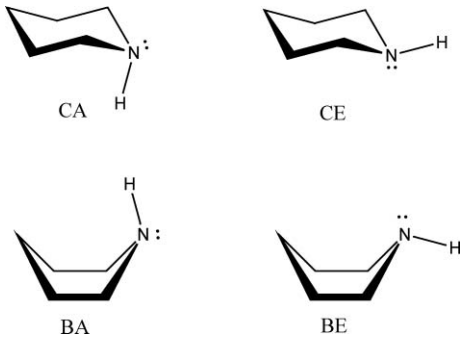

Fig. 3 Potential conformers for piperidine (CA = chair, axial H; CE = chair, equatorial H; BA = boat, axial H; BE = boat, equatorial H).

The structure of $[Ni_2(\mathbf{L}^1)_2(pipi)_4]\cdot pipi$ (R = *t*-Bu) (Fig. 4) reveals an arrangement largely similar to that observed previously for the complexes of type $[M_2(\mathbf{L}^1)_2(EtPy)_4]$ (M = Co(II), Ni(II), Zn(II) (R = *t*-Bu),[11] with the nickel centres each adopting octahedral geometries and separated by 7.469(1) Å. The *β*-diketonato ligands are again close to planar with the oxygen donors occupying the equatorial plane and the piperidine ligands coordinated axially. However, in contrast to the related 4-ethylpyridine adduct species discussed above, there is an additional piperidine solvent molecule present in the lattice, which is strongly hydrogen bonded [N(1)H···N(5), 2.188(13) Å, N(3)H···N(5A) 2.19(2) Å] between two coordinated piperidine molecules on one side of the molecular plane (Fig. 4).

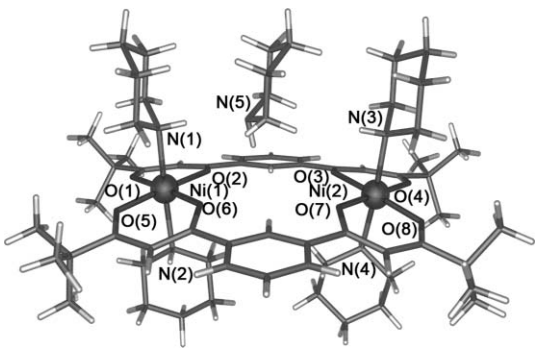

Fig. 4 Perspective representation of the crystal structure of $[Ni_2(\mathbf{L}^1)_2(pipi)_4]\cdot pipi$ (R = *t*-Bu), with disorder not shown for clarity.

Each of the piperidine molecules adopts a chair conformation with the *N*-bound hydrogen in the axial position (this corresponding to the CA conformer) leading to each piperidine being arranged approximately orthogonal to the mean plane of the overall complex molecule. However the piperidine solvate molecule is present in a CE conformation. The coordinated piperidine molecules that are not hydrogen bonded to the piperidine solvate molecule are rotated around each Ni–N bond by nearly 90° relative to the two that are.

In contrast, the structure of $[Cu_2(\mathbf{L}^1)_2(pipi)_2]\cdot pipi$ (R = *t*-Bu) shows that the Cu(II) centres are once again in their apparently preferred five-coordinate geometry with the oxygen donors from the *β*-diketonato ligands occupying the basal plane and coordinated piperidine ligands in apical positions (Fig. 5). As observed in the above structure, each of the piperidine molecules are present in a chair conformation, with the coordinated piperidine ligands

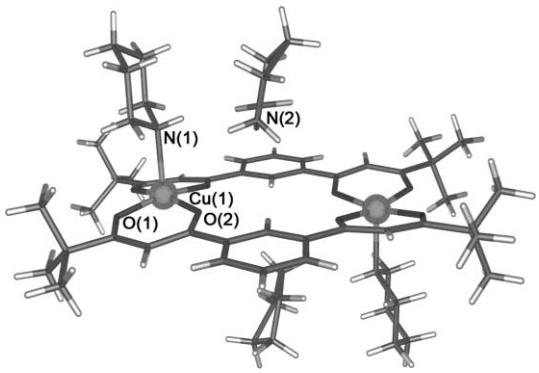

Fig. 5 Perspective representation of the crystal structure of $[Cu_2(\mathbf{L}^1)_2(pipi)_2]\cdot 2pipi$ (R = *t*-Bu), disorder not shown for clarity. Symmetry code used for generating equivalent atoms: 1–x, y, 1–z; x, –y z.

each adopting a CA conformer; both these ligands are hydrogen bound to the piperidine solvate molecules in a similar fashion to that occurring in the above analogous Ni(II)-containing structure [N(1)H···N(2), 2.56(3) Å, N(1)H···N(2A), 2.17(3) Å].

As discussed above and also demonstrated previously for trinuclear species of ligands of type $\mathbf{L}^2$, the reaction of a divalent metal ion with a preference for octahedral geometry such as Co(II) or Ni(II) with ligands of type $\mathbf{L}^1$ or $\mathbf{L}^2$ in the presence of a suitable (potentially monodentate) auxiliary ligand tends to result in six-coordinate metal centres in which the auxiliary ligands occupy *trans* axial positions in the coordination sphere.[11,13,16] If, however, a potentially bidentate ligand coordinates by both donor atoms to a single metal centre, then the *β*-diketonato domains on different $\mathbf{L}^1$ ligands would be required to adopt a mutually *cis*-arrangement around the resulting octahedral centre. This would require the overall bis-*β*-diketonate ligand to twist such that a double helicate could result. The sterically demanding, potentially bidentate ligand, *N*,*N*,*N*′,*N*′-tetramethylethylenediamine (tmen), was employed as the auxiliary ligand to probe this possibility.

$[Co_2(\mathbf{L}^1)_2(tmen)_2]$ (R = *t*-Bu), $[Ni_2(\mathbf{L}^1)_2(tmen)_2]$ (R = *t*-Bu) and $[Cu_2(\mathbf{L}^1)_2(tmen)_2]$ (R = *t*-Bu) were synthesised by dissolving the appropriate starting complex in hot *N*,*N*,*N*′,*N*′-tetramethylethylenediamine, followed by filtration and slow cooling of the solution. The X-ray structures of crystalline $[Co_2(\mathbf{L}^1)_2(tmen)_2]$ (R = *t*-Bu) and $[Ni_2(\mathbf{L}^1)_2(tmen)_2]$ (R = *t*-Bu) obtained in this manner are presented in Fig. 6 and that of $[Cu_2(\mathbf{L}^1)_2(tmen)_2]$ in Fig. 7.

As expected, in $[Co_2(\mathbf{L}^1)_2(tmen)_2]$ (R = *t*-Bu) and $[Ni_2(\mathbf{L}^1)_2(tmen)_2]$ (R = *t*-Bu) the metal centres are again octahedral, however, in contrast to the structure of $[Ni_2(\mathbf{L}^1)_2(pipi)_4]\cdot pipi$ (R = *t*-Bu) and other complexes of $\mathbf{L}^1$ and $\mathbf{L}^2$ with Co(II) or Ni(II),[11,13,16] the *β*-diketonato moieties adopt a *cis*-orientation about the metal centres, with the remaining two coordination sites at each metal centre being occupied by the tertiary nitrogen donors of the tmen ligand.

The above *cis*-coordination has a significant influence on the overall geometry of the respective dinuclear complexes. Unlike the dinuclear structures discussed so far, the geometry of the present complex is helix-like, with the ligands in this case adopting coordination arrangements in which two of the *β*-diketonato oxygens are mutually *trans* in each coordination sphere. The resulting twist originating at the metal centres extends along the

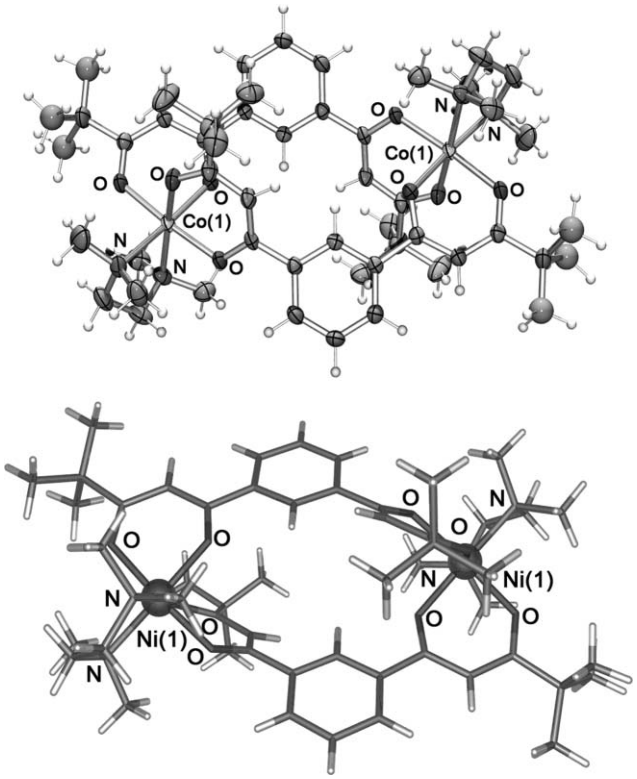

Fig. 6 Top: ORTEP representation of $[Co_2(\mathbf{L}^1)_2(tmen)_2]$ (R = *t*-Bu) shown with 50% probability ellipsoids. Bottom: perspective representation of $[Ni_2(\mathbf{L}^1)_2(tmen)_2]$ (R = *t*-Bu). Disorder not shown for clarity. Symmetry code used for generating equivalent atoms: 1.5–x, $\frac{1}{2}$–y, –z.

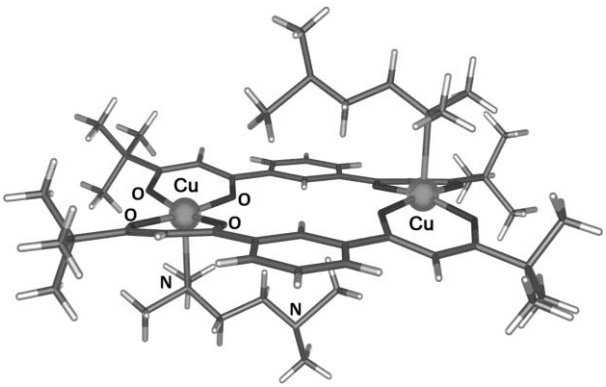

Fig. 7 Perspective representation of $[Cu_2(L^1)_2(tmen)_2]$ (R = *t*-Bu). Disorder not shown for clarity. Symmetry code used for generating equivalent atoms: –x, –y, –z.

length of the molecule. As the molecules are situated around an inversion centre, each complex molecule contains one Λ centre and one Δ centre, such that the overall molecule is not homochiral and thus represents a *meso* isomer and not a true helicate. In this arrangement each $\mathbf{L}^1$ (R = *t*-Bu) is not flat, but has one diketo 'arm' rotated ~35° from the plane of the central phenyl ring (the other lies almost in the plane of this ring, rotated by only 6°). There are no significant interactions between adjacent molecules in the lattice. In contrast, the structure of $[Cu_2(\mathbf{L}^1)_2(tmen)_2]$ (R = *t*-Bu) is markedly different to the above structure, again presumably reflecting the preference of the Cu(II) centres for a five-coordinate distorted square pyramidal geometry. Namely, in $[Cu_2(\mathbf{L}^1)_2(tmen)_2]$ (R = *t*-Bu) a tmen ligand binds to each copper in a monodentate fashion, with the second donor remaining uncoordinated.

The potentially di-functional aliphatic bases 1,4-piperazine (pip), *N*-methylmorpholine (mmorph) and 1,4-dimethylpiperazine (dmpip) (see Scheme 1) were also employed as ancillary ligands in an endeavour to induce the formation of extended systems of the type observed previously for the analogous structures incorporating difunctional aromatic ancillary ligands.[7,8,10,15] It is noted that once again there are a number of conformations possible for these aliphatic heterocyclic ligand systems and the conformer adopted will hence influence the overall structure attained by the corresponding dinuclear amine-containing product.

The interaction of $[Ni_2(\mathbf{L}^1)_2(Py)_4]$ (R = *t*-Bu) with 1,4-dimethylpiperazine (dmpip) was investigated. The nickel complex was dissolved in hot 1,4-dimethylpiperazine; several days of slow evaporation of this solution yielded green prismatic crystals suitable for X-ray diffraction. It was anticipated that the large excess of this tertiary nitrogen base (even though it is somewhat sterically hindered) might promote the displacement of the pyridine ligands in the precursor complex. However, the structural analysis revealed that the $[Ni_2(\mathbf{L}^1)_2(Py)_4]$ (R = *t*-Bu) unit remained intact, with a 1,4-dimethylpiperazine solvent molecule now residing in the crystal lattice (Fig. 8).

The above result undoubtedly reflects the high stability of the pyridine adduct which may also be influenced by the presence of strong π–π interactions in the structure. These interactions differ from those occurring in the corresponding non-solvated pyridyl derivative reported previously.[11] In the latter structure a series of edge-to-face and offset face-to-face interactions result in the formation of motifs resembling molecular "zippers". In the present case a ribbon-like structure occurs (Fig. 9), with two distinct types of π–π interactions occurring in the lattice. The N(1)-containing rings in adjacent molecules (–x, –y, 1–z) interact with nearly idealised face-to-face π–π contacts [N(1)-containing ring centroid separation 3.35 Å, 94°], while the N(2)-containing rings interact with the N(1)-containing rings in an edge-to-face manner [H(29) to the N(1)-containing centroid, 2.73 Å]. The ribbons propagate along the crystallographic *a*-axis and pack closely throughout the lattice leaving small voids which are occupied by the 1,4-dimethylpiperazine molecules. The 1,4-dimethylpiperazine is present in its chair conformer with its methyl groups occupying equatorial positions.

Interaction of $[Cu_2(\mathbf{L}^1)_2(THF)_2]$ (R = *t*-Bu) with 1,4-piperazine yielded green crystals suitable for X-ray diffraction. The structure revealed that this product is of type $\{[Cu_2(\mathbf{L}^1)_2(pip)]\cdot pip\cdot 2THF\}_n$ (R = *t*-Bu) with each Cu(II) centre being five-coordinate and square pyramidal. Four *β*-diketonato oxygen atoms again occupy the basal plane and a secondary nitrogen atom from the 1,4-piperazine ligand is bound in an apical site. Each of the nitrogen-containing ligands bridges two copper centres such that the resulting structure is a one-dimensional stepped polymer (Fig. 10).

The coordinated 1,4-piperazine molecules each adopt a chair (NH axial) conformation resulting in a minimum displacement from linear geometry. A tetrahydrofuran molecule is hydrogen bound to one of these axial hydrogens in a similar manner to that in $\{[Cu_2(\mathbf{L}^1)_2(dpyx)]\cdot 1.7THF\}_n$ (R = *t*-Bu).[9] There is an

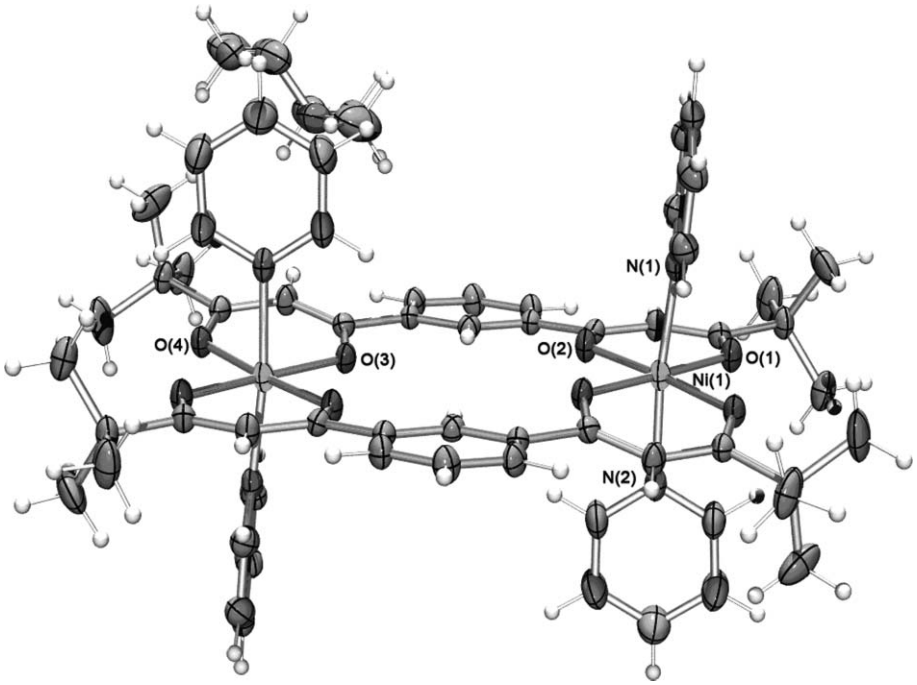

Fig. 8 X-ray structure of $[Ni_2(L^1)_2(Py)_4]$·dmpip (R = *t*-Bu) shown with 50% probability ellipsoids. Symmetry code used to generate equivalent atoms: –x, –y, –z.

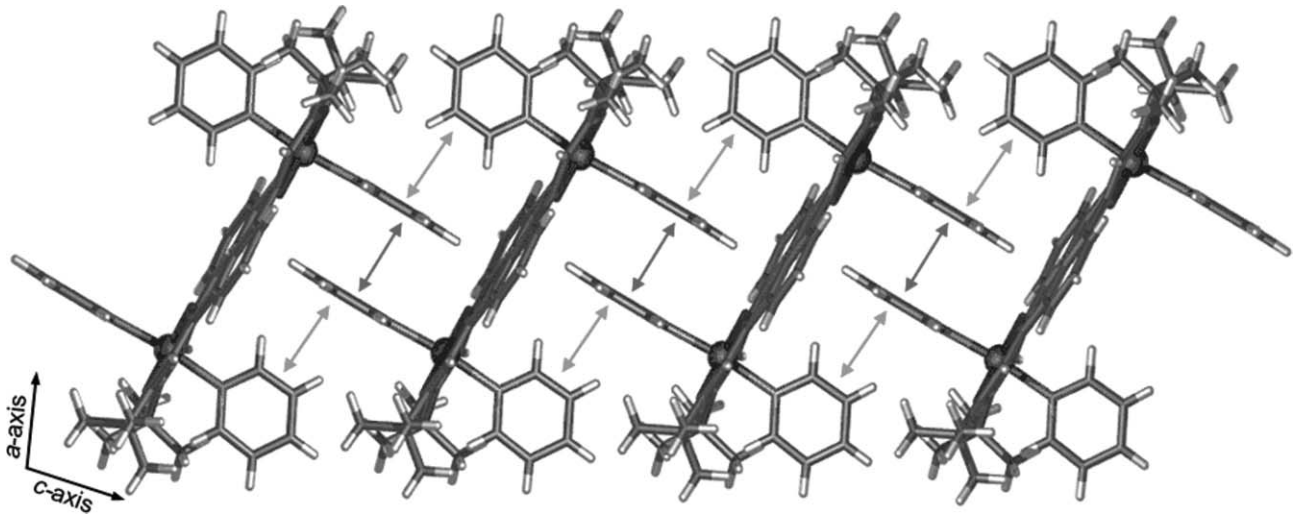

Fig. 9 Perspective representation of a portion of the crystal packing in $[Ni_2(L^1)_2(Py)_4]$·dmpip (R = *t*-Bu). Arrows indicate face-to-face π-stacking and edge-to-face π-interactions. Solvent molecules omitted for clarity.

additional lattice 1,4-piperazine molecule that also adopts a chair conformation. In this case it proved not possible to locate the nitrogen-bound hydrogen atoms in the Fourier difference map and so they were not modelled in the X-ray refinement. Overall, each of the one-dimensional chains are arranged adjacent to one other, slightly offset, and are held together by weak offset face-to-face π–π stacking interactions (with relevant C···C distances of 3.5–3.8 Å). This results in the overall structure being an infinite undulating two-dimensional polymer, with the solvent and uncoordinated 1,4-piperazine molecules occupying the voids in the lattice.

$[Cu_2(\mathbf{L}^1)_2]$ (R = *t*-Bu) was dissolved in *N*-methylmorpholine and slow evaporation of the green solution resulted in the formation of X-ray quality crystals. It was anticipated that the tertiary nitrogen of the *N*-methylmorpholine would likely coordinate to an apical site of each Cu(II) centre, with the possibility that the *N*-methylmorpholine ether oxygen donor might also bind to an adjacent copper to form either a discrete tetranuclear complex or an extended ribbon/ladder-like polymer.

The X-ray structure of $[(Cu_2(\mathbf{L}^1)_2(mmorph)_2]$ (R = *t*-Bu) is given in Fig. 11 and a perspective representation of part of the crystal packing is shown in Fig. 12. The structure is disposed about a crystallographic inversion centre and is similar to those obtained for the monodentate base adducts described above and previously.[7,9,11] That is, the Cu(II) ions are once again five-coordinate and square pyramidal, with the tertiary nitrogen of

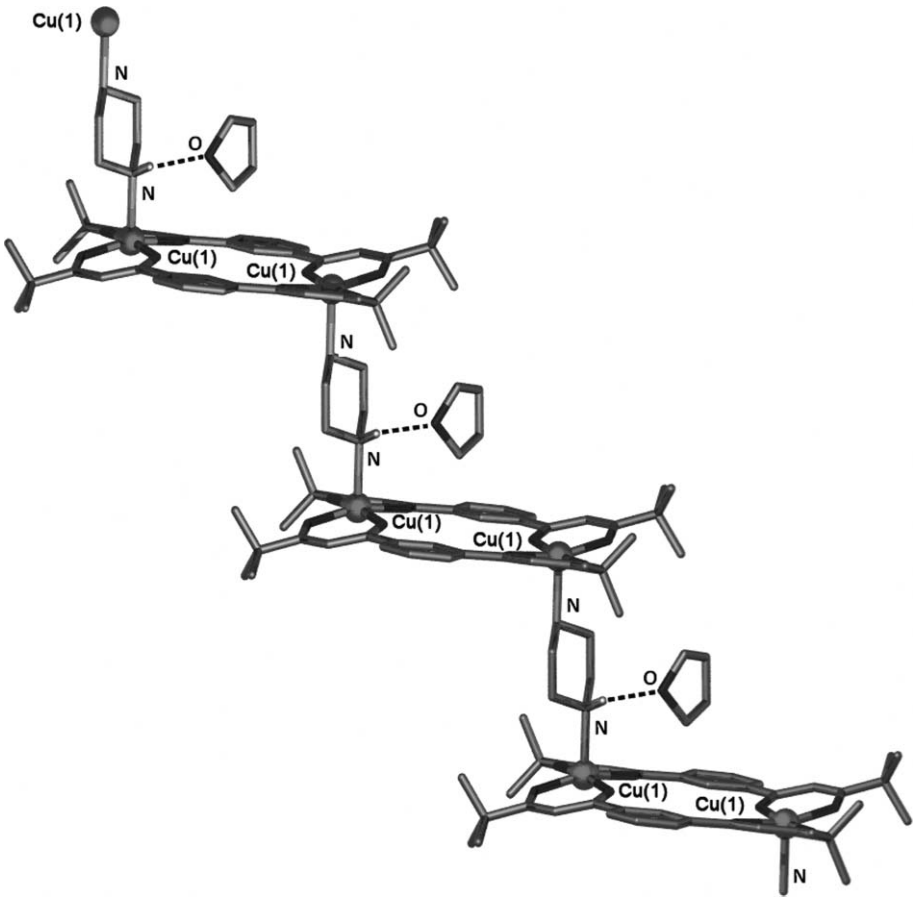

Fig. 10 Perspective representation of a fragment of the one-dimensional chain in $\{[Cu_2(\mathbf{L}^1)_2(pip)]\cdot pip\cdot 2THF\}_n$ (R = *t*-Bu) showing the hydrogen bonded THF molecules. Hydrogen atoms and free piperazine molecules removed for clarity.

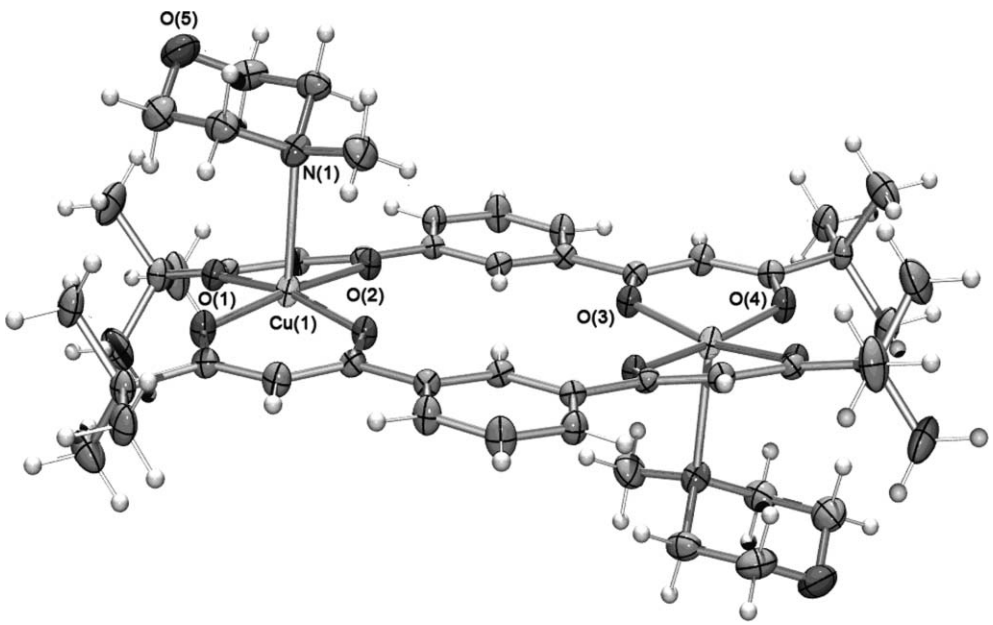

Fig. 11 ORTEP representation of $[(Cu_2(\mathbf{L}^1)_2(mmorph)_2]$ (R = *t*-Bu) with 50% probability ellipsoids. Symmetry code used for generating equivalent atoms: –x, 1–y, –z.

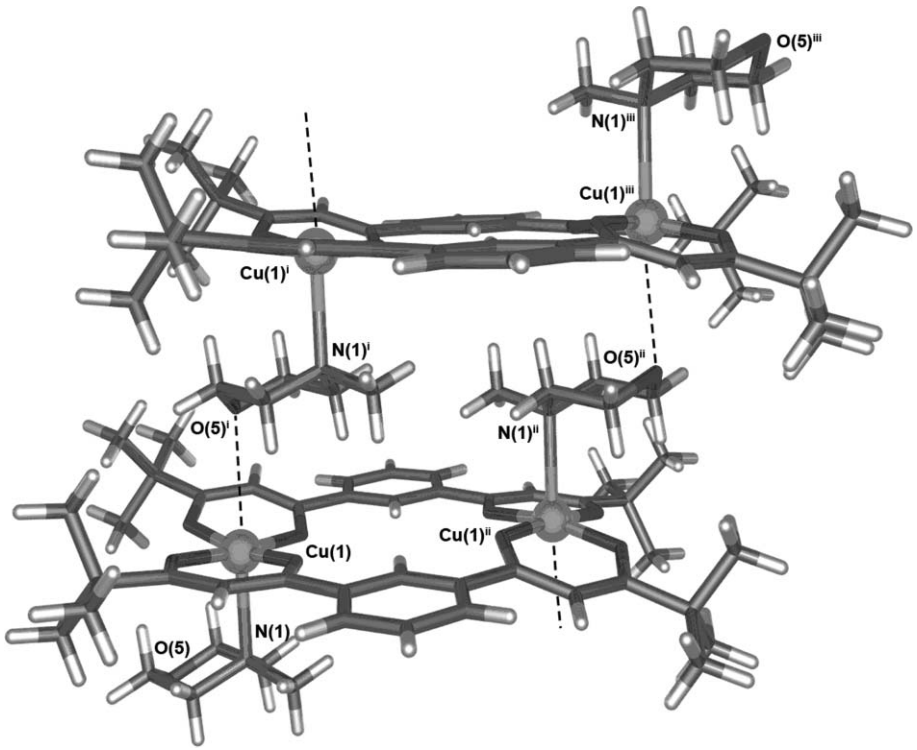

Fig. 12 Perspective representation of part of the packing in $[(Cu_2(\mathbf{L}^t)_2(mmorph)_2]$ (R = *t*-Bu). Dashed lines indicate Cu–O contacts. Symmetry codes used for generating equivalent atoms: [i] –x, 1–y, –z, [ii] 1–x,1–y,–z, [iii]2–x, 1–y, z.

N-methylmorpholine coordinated in the apical position at each metal centre and the *β*-diketonato oxygens occupying the square base of the pyramidal copper centres. The copper–nitrogen bond lengths are longer [2.492(2) Å] than those in the related pyridine-containing adduct [2.2781(17) Å].[7]

The coordinated *N*-methylmorpholine ring in the above complex resides in a chair conformer with the methyl group in an equatorial position. In contrast to the previous structures, adjacent complexes pack directly above each other in close proximity (in the structures discussed previously they were offset reflecting the presence of π–π interactions) forming a stack in the crystallographic *a* direction; there is no residual solvent in the lattice. Long intermolecular Cu(II)–ether oxygen distances [3.364(7) Å] are present (Fig. 12). Although these contacts are too long to be considered formal bonds, they likely contribute to the stability of the overall structure even though each ether oxygen atom is slightly displaced from the ideal position for an apical donor *trans* to the coordinated nitrogen atom [(N(1)–Cu(1), 2.536(6) Å; O(5)[i]–Cu(1), 3.364(7) Å; N(1)–Cu(1)–O(5)[i], 167.7(2)°]; repetition of the above motif leads to an extended loose ribbon-like arrangement throughout the lattice (Fig. 12). The Cu–Cu distances are 7.456(4) Å within each building block [Cu(1)–Cu(1)[ii]] and are 7.108(4) Å between adjacent platforms [Cu(1)–Cu(1)[iii]] with a Cu(1)–Cu(1)[ii]–Cu(1)[iii] angle of 110.1(1)° There are also some very weak offset face-to-face π–π interactions between adjacent stacks in the lattice extending in the crystallographic *b* direction, illustrated by a stacking separation of 3.35 Å. In part, the presence of the long Cu · · · O contacts mentioned above motivated an investigation of the effect of pressure on the ambient pressure structure. In particular, it was of interest to investigate whether the application of pressure would result in solid state compression, leading to formation of a polymeric species in which adjacent platforms approached each other more closely, perhaps linked by shorter Cu · · · O interactions.

High pressure study of $[Cu_2(L^t)_2(mmorph)_2]$ (R = *t*-Bu)

A single crystal of $[Cu_2(\mathbf{L}^t)_2(mmorph)_2]$ (R = *t*-Bu) was loaded into a diamond anvil cell using paraffin as the hydrostatic medium. X-ray data were collected at 1.9 kbar and 9.1 kbar employing synchrotron radiation. Attempts to increase the pressure beyond 9.1 kbar resulted in loss of crystallinity of the sample.

The application of pressure resulted in small changes in unit cell parameters and also a corresponding decrease in the unit cell volume. At 9.1 kbar, the *a*-axis had decreased by 2.4% [from 6.9932(11) Å to 6.8237(5) Å], the *b*-axis by 2.2% [from 11.2678(18) Å to 11.0237(8) Å] and the *c*-axis by 2.5% [from 16.466(7) Å to 16.053(3) Å] when compared to the unit cell obtained at 1.9 kbar, there are also small increases in the unit-cell angles. These correspond to a decrease in the cell volume of 6.7% [from 1233.6(6) $Å^3$ to 1151.3(3) $Å^3$]. In this pressure range the symmetry is maintained and there is no phase transition observed.

Changes in a number of inter-atomic distances and angles are observed. The Cu–ether oxygen [Cu(1)–O(5)[i]] distance mentioned above decreases from 3.364(7) Å in the ambient structure to 3.077(7) Å in the 9.1 kbar structure, while the N(1)–Cu(1)–O(5)[i] angles remain almost the same. The Cu(1)–N(1) bond compresses slightly from 2.536(6) Å to 2.444(7) Å. The offset face-to-face π–π stacking distance decreases from 3.35 to 3.22 Å resulting in stronger interactions. At the higher pressure there are a number

of 'close contacts' within the structure; for example, between the methylene hydrogen atoms in the *N*-methylmorpholine ligands and the *β*-diketonato rings as well as between adjacent *t*-butyl groups. In the ambient structure the copper–copper distances are 7.456(4) Å within each building block [Cu(1)–Cu(1)^{ii}] and 7.108(4) Å between the nearest copper atoms in adjacent parallel platforms [Cu(1)–Cu(1)^{iii}], with a Cu(1)–Cu(1)^{ii}–Cu(1)^{iii} angle of 110.1(1)°. At 9.1 kbar these distances have decreased to 7.419(2) Å and 6.824(1) Å respectively, while the Cu(1)–Cu(1)^{ii}–Cu(1)^{iii} angle has increased to 111.4(1)°. The changes in molecular geometry overall are slight; no new bonds are formed, no bonds are broken and overall the structure can still be described as a loose ribbon-like arrangement involving adjacent discrete dinuclear complex units. Nevertheless, it should be noted that a minor 'shearing' between adjacent building blocks occurs throughout the lattice. The adjacent complexes shift slightly with respect to each other along the *c*-axis. This leads to the increase in the Cu(1)–Cu(1)^{ii}–Cu(1)^{iii} angle mentioned above and reflects the reduction of the void volumes within the structure which has also been observed in the structures of a number of small organic molecules.[35] The voids (shaded) in the ambient pressure (left) and highest pressure (right) structures are shown in Fig. 13. The most significant voids are concentrated between the phenylene rings within a stack and in the gaps formed at the corners of four adjacent stacks, proximal to the tertiary butyl groups.

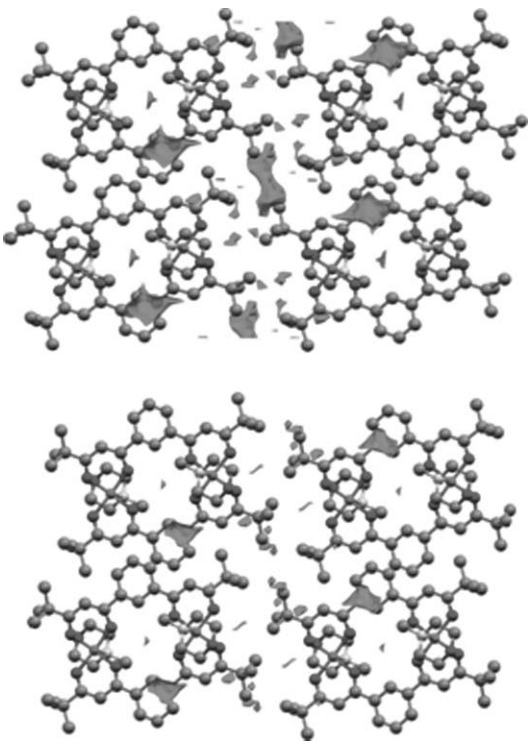

Fig. 13 View along the crystallographic *a*-axis in the ambient (top) and 9.1 kbar (below) structures of $[Cu_2(L^1)_2(mmorph)_2]$ (R = *t*-Bu). Voids are represented by the shaded areas; those adjacent to the tertiary butyl groups, namely between adjacent stacks, can be seen to close up significantly.

At ambient pressure there is disorder in one of the crystallographically independent tertiary butyl groups which disappears as pressure is applied and the adjacent void closes up. However, the void found between the aromatic rings appears more resistant to pressure and does not reduce to the same extent.

Concluding remarks

New discrete and polymeric structures based on dinuclear Cu(II) complexes of aryl-linked bis-*β*-diketonates can be readily generated through axial ligand exchange on reaction with an appropriate ancillary mono- or di-functional amine ligand. Related procedures can also be employed to form similar dinuclear Co(II) and Ni(II) adducts. An X-ray diffraction study shows that when high pressure is applied to $[Cu_2(\mathbf{L}^1)_2(mmorph)_2]$ (R = *t*-Bu) a major reduction in void volume occurs, corresponding to a decrease in cell volume of 6.7% at 9.1 kbar from that at ambient pressure; removal of the disorder associated with the pendant *t*-butyl groups is also observed.

Acknowledgements

We acknowledge the Australian Research Council, The Engineering and Physical Sciences Research Council (UK), EaStCHEM and Infineum Ltd. for support. L.F.L thanks The Royal Society of Chemistry for the award of a Journal Grant for International Authors for a visit to The University of Edinburgh in support of the Sydney/Edinburgh collaborative investigation reported in this manuscript. JKC acknowledges the receipt of a Joan R. Clark scholarship from the University of Sydney in support of this project.

References

1 A. Werner, *Ber. Dtsch. Chem. Ges.*, 1901, **34**, 2594; A. G. Swallow and M. R. Truter, *Proc. R. Soc. London, Ser. A*, 1960, **254**, 205; D. Gibson, *Coord. Chem. Rev.*, 1969, **4**, 225; F. P. Dwyer and D. P. Mellor, *Chelating Agents and Metal Chelates*, Academic Press, London, 1964; U. Casellato, P. Vigato and M. Vivaldi, *Coord. Chem. Rev.*, 1977, **23**, 31; U. Casellato, *Chem. Soc. Rev.*, 1979, **8**, 199.

2 See, for example: D. V. Soldatov, *J. Chem. Crystallogr.*, 2006, **36**, 747; D. J. Bray, J. K. Clegg, L. F. Lindoy and D. Schilter, *Adv. Inorg. Chem.*, 2006, **59**, 1; T.-J. Won, J. K. Clegg, L. F. Lindoy and J. C. McMurtrie, *Cryst. Growth Des.*, 2007, **7**, 972 and refs. therein; G. Aromi, P. Gamez and J. Reedijk, *Coord. Chem. Rev.*, 2008, **252**, 964; J. K. Clegg, K. A. Jolliffe, L. F. Lindoy and G. V. Meehan, *Polish J. Chem.*, 2008, **82**, 1131.

3 R. W. Saalfrank, N. Low, B. Demleitner, D. Stalke and M. Teichert, *Chem.–Eur. J.*, 1998, **4**, 1305and refs. therein; R. W. Saalfrank, V. Seitz, F. W. Heinemann, C. Göbel and R. Herbst-Irmer, *J. Chem. Soc., Dalton Trans.*, 2001, 599.

4 R. W. Saalfrank, C. Schmidt, H. Maid, F. Hampel, W. Bauer and A. Scheuer, *Angew. Chem., Int. Ed.*, 2006, **45**, 315.

5 See, for example: G. Aromi, P. Gamez, O. Roubeau, P. C. Berzal, H. Kooijman, A. L. Spek, W. L. Driessen and J. Reedijk, *Inorg. Chem.*, 2002, **41**, 3673; G. Aromi, P. Gamez, P. C. Berzal, W. L. Driessen and J. Reedijk, *Synth. Commun.*, 2003, **33**, 11; M. Albrecht, S. Schmid, M. deGroot, P. Weis and R. Fröhlich, *Chem. Commun.*, 2003, 2526; G. Aromí, H. Stoeckli-Evans, S. J. Teat, J. Cano and J. Ribas, *J. Mater. Chem.*, 2006, **16**, 2635; G. Aromí, C. Boldron and P. Gaez, *Dalton Trans.*, 2004, 3586; O. Roubeau, H. Kooijman, A. L. Spek, H. Stoeckli-Evans, J. Ribasa, J. Reedijk, G. Aromí, J. Ribas, P. Gamez, O. Roubeau, H. Kooijman, A. L. Spek, S. Teat, E. MacLean, H. Stoeckli-Evans and J. Reedijk, *Chem.–Eur. J.*, 2004, **10**, 6476; A. P. Bassett, S. W. Magennis, P. B. Glover, D. J. Lewis, N. Spencer, S. Parsons, R. M. Williams, L. De Cola and Z. Pikramenou, *J. Am. Chem. Soc.*, 2004, **126**, 9413; Bai-Shu Zheng, Xiao-Yi Zhang, Huai-Wu Zhu, Shi-Xia Luo, L. F. Lindoy, J. C. McMurtrie, P. Turner and G. Wei, *Dalton Trans.*, 2005, 1349; S. N. Podyachev, I. A. Litvinov, A. R. Mustafina, R. R. Shagidullin, W. D. Habicher and A. I. Konovalov, *Russ. Chem. Bull.*, 2005, **54**, 623; G. Aromi, P. Gamez, C. Boldron, H. Kooijman, A. L. Spek and J.

Reedijk, *Eur. J. Inorg. Chem.*, 2006, 1940; X. Zhang, H. Chen, C. Ma, C. Chen and Q. Liu, *Dalton Trans.*, 2006, 4047; M. Albrecht, S. Dehn, S. Schmid and M. DeGroot, *Synthesis*, 2007, 155; T. Shiga, N. Ito, A. Hidaka, H. Ōkawa, S. Kitagawa and M. Ohba, *Inorg. Chem.*, 2007, **46**, 3492; G. Aromi, P. Gamez, J. Krzystek, H. Kooijman, A. L. Spek, E. J. MacLean, S. J. Teat and H. Nowell, *Inorg. Chem.*, 2007, **46**, 2519; C. Pariya, C. R. Sparrow, C.–K. Back, G. Sandi, F. R. Fronczek and A. W. Maverick, *Angew. Chem.*, 2007, **119**, 6421.

6 J. K. Clegg, L. F. Lindoy, B. Moubaraki, K. S. Murray and J. C. McMurtrie, *Dalton Trans.*, 2004, 2417; J. K. Clegg, S. S. Iremonger, M. J. Hayter, P. D. Southon, R. B. Macquart, M. B. Duriska, P. Jensen, P. Turner, K. A. Jolliffe, C. J. Kepert, G. V. Meehan and L. F. Lindoy, *Angew. Chem., Int. Ed.*, 2010, **49**, 1075.

7 J. K. Clegg, L. F. Lindoy, J. C. McMurtrie and D. Schilter, *Dalton Trans.*, 2005, 857.

8 J. K. Clegg, L. F. Lindoy, J. C. McMurtrie and D. Schilter, *Dalton Trans.*, 2006, 3114.

9 J. K. Clegg, K. Gloe, M. J. Hayter, O. Kataeva, L. F. Lindoy, B. Moubaraki, J. C. McMurtrie, K. S. Murray and D. Schilter, *Dalton Trans.*, 2006, 3977.

10 J. K. Clegg, *Aust. J. Chem.*, 2006, **59**, 660.

11 J. K. Clegg, D. J. Bray, K. Gloe, K. Gloe, M. J. Hayter, K. A. Jolliffe, G. A. Lawrance, G. V. Meehan, J. C. McMurtrie, L. F. Lindoy and M. Wenzel, *Dalton Trans.*, 2007, 1719.

12 D. J. Bray, K. A. Jolliffe, L. F. Lindoy and J. C. McMurtrie, *Tetrahedron*, 2007, **63**, 1953.

13 J. K. Clegg, D. J. Bray, K. Gloe, K. Gloe, K. A. Jolliffe, G. A. Lawrance, L. F. Lindoy, G. V. Meehan and M. Wenzel, *Dalton Trans.*, 2008, 1331.

14 D. J. Bray, B. Antonioli, J. K. Clegg, K. Gloe, K. Gloe, K. A. Jolliffe, L. F. Lindoy, G. Wei and M. Wenzel, *Dalton Trans.*, 2008, 1683.

15 D. V. Soldatov, I. E. Sokolov and K. Sowin'ska, *J. Struct. Chem.*, 2005, **46**, S158; D. V. Soldatov, G. D. Enright and I. E. Sokolov, *J. Struct. Chem.*, 2007, **48**, 325.

16 D. V. Soldatov, A. S. Zanina, G. D. Enright, C. I. Ratcliffe and J. A. Ripmeester, *Cryst. Growth Des.*, 2003, **3**, 1005.

17 *Bruker, SMART, SAINT and XPREP*, 1995, Bruker Analytical X-ray Instruments Inc., Madison, Wisconsin, USA .

18 *Bruker-Nonius, APEX v2.1, SAINT v.7 and XPREP v.6.14*, 2003, Bruker AXS Inc. Madison, Wisconsin, USA.

19 *Bruker-Nonius, APEX v2.1, SAINT v.7 and XPREP v.6.14*, 2003, Bruker AXS Inc. Madison, Wisconsin, USA.

20 WinGX-32: System of programs for solving, refining and analysing single crystal X-ray diffraction data for small moleculesL. J. Farrugia, *J. Appl. Crystallogr.*, 1999, **32**, 837.

21 A. Altomare, M. C. Burla, M. Camalli, G. L. Cascarano, C. Giocavazzo, A. Guagliardi, A. G. C. Moliterni, G. Polidori and S. Spagna, *J. Appl. Crystallogr.*, 1999, **32**, 115.

22 G. M. Sheldrick, *SADABS: Empirical Absorption and Correction Software*, University of Göttingen, Germany, 1999-2006.

23 G. M. Sheldrick, *SHELXL-97: Programs for Crystal Structure Analysis*, University of Göttingen, Germany, 1997.

24 L. Merrill and W. A. Bassett, *Rev. Sci. Instrum.*, 1974, **45**, 290.

25 G. J. Piermarini, S. Block, J. D. Barnett and R. A. Forman, *J. Appl. Phys.*, 1975, **46**, 2774.

26 A. Dawson, D. R. Allan, S. Parsons and M. Ruf, *J. Appl. Crystallogr.*, 2004, **37**, 410; D. R. Allan, S. Parsons and S. J. Teat, *J. Synchrotron Radiat.*, 2001, **8**, 10.

27 S. Parsons, *SHADE*, The University of Edinburgh, UK, 2004.

28 R. H. Blessing, *Acta Crystallogr., Sect. A: Found. Crystallogr.*, 1995, **A51**, 33.

29 R. H. Blessing, *J. Appl. Crystallogr.*, 1997, **30**, 421.

30 P. W. Betteridge, J. R. Carruthers, R. I. Cooper, K. Prout and D. J. Watkin, *J. Appl. Crystallogr.*, 2003, **36**, 1487.

31 L. F. Lindoy and I. M. Atkinson, *Self-Assembly in Supramolecular Systems*, Cambridge, UK, 2000.

32 P. J. Steel, *Acc. Chem. Res.*, 2005, **38**, 243.

33 See for example: H. M. Pickett and H. L. Strauss, *J. Am. Chem. Soc.*, 1970, **92**, 7281; B. Chiari, O. Piovesana, T. Tarantelli and P. D. Zanazzi, *Acta Crystallogr., Sect. B: Struct. Crystallogr. Cryst. Chem.*, 1982, **B38**, 331; M. Kuppayee, D. Kumaran, M. N. Ponnuswamy, M. Kandaswamy, M. J. Violet, K. Chinnakali and H. -K. Fun, *Acta Crystallogr., Sect. C: Cryst. Struct. Commun.*, 1999, **C55**, 2147; F. G. Mann and H. R. Watson, *J. Chem. Soc.*, 1958, 2772.

34 M. Boiocchi, M. Bonizzoni, L. Fabbrizzi, F. Foti, M. Licchelli, A. Taglietti and M. Zema, *Dalton Trans.*, 2004, 653; K. Kubono, N. Hirayama, H. Kokusen and K. Yokoi, *Anal. Sci.*, 2003, **19**, 645; A. Marzotto, D. A. Clemente and G. Valle, *Acta Crystallogr., Sect. C: Cryst. Struct. Commun.*, 1997, **C53**, 1580; J. Ratilainen, K. Airola, R. Frölich, M. Niegar and K. Rissanen, *Polyhedron*, 1999, **18**, 2265; O. Hassel and B. F. Pedersen, *Proc. Chem. Soc.*, 1959, 394.

35 S. A. Moggach, D. R. Allan, S. J. Clark, M. J. Gutmann, S. Parsons, C. R. Pulham and L. Sawyer, *Acta Crystallogr., Sect. B: Struct. Sci.*, 2006, **B62**, 296; S. A. Moggach, W. G. Marshall and S. Parsons, *Acta Crystallogr., Sect. B: Struct. Sci.*, 2006, **B62**, 815; F. P. A. Fabbiani, D. R. Allan, S. Parsons and C. R. Pulham, *Acta Crystallogr., Sect. B: Struct. Sci.*, 2006, **B62**, 826; P. A. Wood, R. S. Forgan, D. Henderson, S. Parsons, E. Pidcock, P. A. Tasker and J. E. Warren, *Acta Crystallogr., Sect. B: Struct. Sci.*, 2006, **B62**, 1099; S. A. Moggach, D. R. Allan, C. A. Morrison, S. Parsons and L. Sawyer, *Acta Crystallogr., Sect. B: Struct. Sci.*, 2005, **B61**, 58.